Monthly Notices
of the
ROYAL ASTRONOMICAL SOCIETY

Mon. Not. R. Astron. Soc. **403,** 378–386 (2010) doi:10.1111/j.1365-2966.2009.16121.x

Analysis of *RXTE*-PCA Observations of SMC X-1

S. Ç. İnam,[1⋆] A. Baykal[2⋆] and E. Beklen[2,3]

[1]*Department of Electrical and Electronics Engineering, Başkent University, 06530 Ankara, Turkey*
[2]*Physics Department, Middle East Technical University, 06531 Ankara, Turkey*
[3]*Physics Department, Süleyman Demirel University, 32260 Isparta, Turkey*

Accepted 2009 November 25. Received 2009 November 25; in original form 2009 October 6

ABSTRACT

We present timing and spectral analysis of *Rossi X-ray Timing Explorer*-Proportional Counter Array observations of SMC X-1 between 1996 January and 2003 December. From observations around 1996 August 30 with a time-span of ∼6 d, we obtain a precise timing solution for the source and resolve the eccentricity as 0.00089(6). We find an orbital decay rate of $\dot{P}_{\rm orb}/P_{\rm orb} = -3.402(7) \times 10^{-6}\,{\rm yr}^{-1}$ which is close to the previous results. Using our timing analysis and the previous studies, we construct a ∼30 yr long pulse period history of the source. We show that frequency derivative shows long- (i.e. more than a few years) and short-term (i.e. order of days) fluctuations. From the spectral analysis, we found that all spectral parameters except Hydrogen column density showed no significant variation with time and X-ray flux. Hydrogen column density is found to be higher as X-ray flux gets lower. This may be due to the increase in soft absorption when the pulsar is partially obscured as in Her X-1 or may just be an artefact of the tail of a soft excess in energy spectrum.

Key words: accretion, accretion discs – stars: neutron – pulsars: individual: SMC X-1 – X-rays: binaries.

1 INTRODUCTION

The high-mass X-ray binary (HMXB) system SMC X-1/Sk 160 consists of a neutron star with a mass of ∼1.06 $M_\odot$ (van der Meer et al. 2007) and a spin period of 0.71 s (Lucke et al. 1976), accreting from the B0I star Sk 160 with a mass of ∼17.2 $M_\odot$ (Reynolds et al. 1993). Orbital period of the system is ∼3.9 d (Schreier et al. 1972). The system has been observed with several observatories since it was discovered during a rocket flight (Price et al. 1971). It is the only discovered HMXB with a supergiant companion in SMC so far (Galache et al. 2008).

From the pulse timing studies, the source was observed to be spinning up since it was discovered (Wojdowski, Clark George & Levine Alan 1998). Levine et al. (1993) and Wojdowski et al. (1998) found an orbital period decay in the system with $P_{\rm orb}/\dot{P}_{\rm orb}$ of $\sim 3.4 \times 10^{-6}\,{\rm yr}^{-1}$.

SMC X-1 also exhibits super-orbital X-ray flux variations like the 35-d cycle of Her X-1 (Gruber & Rothschild 1984). Average super-orbital period of the source is ∼55 d (Wojdowski et al. 1998; Trowbridge, Nowak & Wilms 2007). The super-orbital X-ray flux variations of SMC X-1 are thought to be due to the precession of a warped accretion disc (Wojdowski et al. 1998).

In this paper, we present timing and spectral analysis of *Rossi X-ray Timing Explorer* (*RXTE*) observations of SMC X-1 between 1996 January and 2003 December. In the next section, we give brief information about instruments and observations. In Section 3, we present the results of timing analysis, including pulse period history and timing solution of the source. In Section 4, X-ray spectral analysis of the source is presented.

⋆E-mail: inam@baskent.edu.tr (SÇİ); elif@astroa.physics.metu.edu.tr (AB)

2 INSTRUMENTS AND OBSERVATIONS

We analysed data from Proportional Counter Array (PCA) on board *RXTE* (Jahoda et al. 1996) of SMC X-1 between 1996 January and 2003 December (MJD 500 93−529 88).

The *RXTE*-PCA consists of an array of five Proportional Counters (PCU) operating in the 2–60 keV energy range, with a total effective area of approximately 7000 cm^2 and a field of view of ∼1° full width at half-maximum. Data obtained from top xenon layers (L1 and R1) of PCUs were used to maximize signal over noise (S/N) in the 3–20 keV energy band. For the observations after 2000 May, for which the propane layer for PCU0 was lost, data obtained from PCU0 were not used in the spectral analysis.

Out of 167 total pointings, we excluded X-ray eclipses (due to low count statistics) and used data obtained from ∼130 pointings with a total exposure of ∼250 ks for the timing analysis. Other than the public observations, the principal investigators of these observations are S. Eikenberry, W. Heindl, D. Chakrabarty, G. W. Clark and J. Deeter. During the observations between 1998 October 16 and 1998 November 24, with an exposure of ∼23 ks, the data were contaminated due to the outburst of the nearby transient X-ray pulsar XTEJ0111.2-7317 (Chakrabarty et al. 1998). We did not use these observations in the X-ray spectral analysis. In order to obtain

© 2010 The Authors. Journal compilation © 2010 RAS

Downloaded from https://academic.oup.com/mnras/article-abstract/403/1/378/1018921 by Middle East Technical University Library user on 24 July 2020

Table 1. Timing solution of SMC X-1.

Parameters	Model (this work)
Timing epoch (MJD)	503 26.623 56961(9)
ν (Hz)	1.413630801(4)
$\dot{\nu}$ (10^{-11} Hz s^{-1})	3.279(5)
Orbital Period (d)	3.89220909(4)
a/c sin I (lt-s)	53.4876(9)
Orbital Epoch	MJD 503 24.691 861(8)
$\dot{P}_{\rm orbit}/P_{\rm orbit}$ (10^{-6} yr^{-1})	−3.402(7)
Eccentricity	0.00089(6)
w (longitude of periastron)	166(12)

the timing solution of the source, we used observations with the proposal number 10139 covering a time-span of about 6 d. These observations are more suitable than other observations to obtain the timing solution, since they are the only set of observations that continuously cover near two orbital periods.

3 TIMING ANALYSIS

For the timing analysis, we generated light curves (3–20 keV) with 0.035-s timing resolution using Good Xenon data. These light curves were background-corrected with a 16-s binned background light curve constructed using background estimator models from the *RXTE* team (URL: ftp://legacy.gsfc.nasa.gov/xte/calib_data/pca_bkgd/). The resulting light curves were corrected to the barycentre of the Solar system. A template pulse profile from each *RXTE* observation was constructed by folding the data on the period which had the greatest power in the periodogram. Pulse arrival times were found by cross-correlating the pulse profiles obtained from ∼200 s long segments with the template pulse profile. Both the template and cross-correlated pulse profiles consisted of 20 phase bins. Cross-correlation was performed by using the harmonic representation of pulse profiles (Deeter & Boynton 1985). In order to obtain pulse arrival times, the pulse profiles were expressed in terms of harmonic series and cross-correlated with the template pulse profile.

3.1 Timing solution

Initially, we found pulse arrival times obtained from a series of observations with a time-span of ∼6 d around MJD 503 24.7. These pulse arrival times can be fitted to an expression to obtain timing solution (Deeter, Boynton & Pravdo 1981). We firstly assumed a

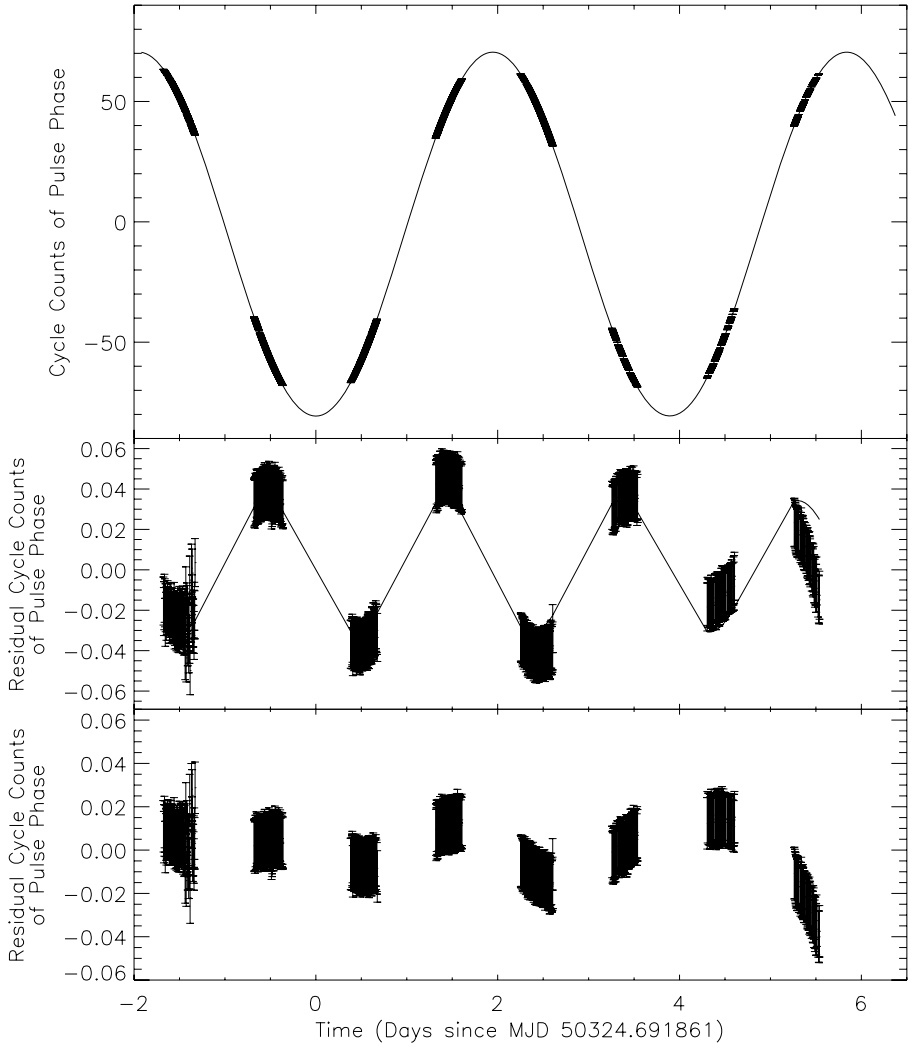


Figure 1. Arrival times (pulsation cycles) (top panel) and residuals after fitting arrival times to a circular (middle panel) and elliptical orbital model (lower panel) obtained from the observations with a time-span of about 6 d around 1996 August 30.

© 2010 The Authors. Journal compilation © 2010 RAS, MNRAS **403,** 378–386

Downloaded from https://academic.oup.com/mnras/article-abstract/403/1/378/1018921 by Middle East Technical University Library user on 24 July 2020

Table 2. Orbital epoch measurements of SMC X-1.

$T_{\pi/2}$ (MJD)	N	Observatory	Reference
409 63.99(2)	−481	*Uhuru*	1,2
422 75.65(4)	−144	*Copernicus*	1,3
428 36.1828(2)	0	*SAS-3*	1,4
429 99.6567(16)	42	*Ariel V*	1,5
431 16.4448(22)	72	*COS-B*	1,6
469 42.472 37(15)	1055	*Ginga*	1,7
474 01.744 476(7)	1173	*Ginga*	1,7
477 40.359 06(3)	1260	*Ginga*	1,7
485 34.347 86(35)	1464	*ROSAT*	1
491 02.591 09(82)	1610	*ASCA*	1
491 37.619 11(50)	1619	*ROSAT*	1
500 91.170(63)	1864	*RXTE*	1
503 24.691 861(8)	1924	*RXTE*	8

References: (1) Wojdowski et al. (1998); (2) Schreier et al. (1972); (3) Tuohy & Rapley (1975); (4) Primini (1977); (5) Davison (1977); (6) Bonnet-Bidaud & van der Klis (1981); (7) Levine et al. (1993); (8) this work.

circular orbit ($e = 0$) and therefore this expression became

$$\delta t = \frac{\delta P}{P}(t - t_0) + \frac{1}{2}\frac{\dot{P}}{P}(t - t_0)^2 + x\,\sin(l). \quad (1)$$

Here, t_0 is the mid-time of the observation, δP is the deviation from mean pulse period, $\dot{P}$ is the time derivative of the pulse period, $x = a/c\,\sin(i)$ is the light traveltime for projected semimajor axis (where i is the inclination angle between the line of sight and the orbital angular momentum vector), $l = 2\pi(t - T_{\pi/2})/P_{\rm orbit} + \pi/2$ is the mean orbital longitude at t, $T_{\pi/2}$ is the epoch when the mean orbital longitude is equal to 90° and $P_{\rm orbit}$ is the orbital period of the system. In order to improve the fit, we used the whole expression containing terms corresponding to an eccentric orbit as

$$\delta t = \frac{\delta P}{P}(t - t_0) + \frac{1}{2}\frac{\dot{P}}{P}(t - t_0)^2 + x\,\sin(l) - \frac{3}{2}xe\sin(w) + \frac{1}{2}xe\cos(w)\sin(2l) - \frac{1}{2}xe\sin(w)\cos(2l). \quad (2)$$

In equation (2), e is the eccentricity and w is the longitude of periastron. The periodic trend of the pulse arrival times yields an eccentric orbit [$e = 0.00089(6)$] with an orbital period of 3.89220909(4) d (numbers in parenthesis denote 1σ uncertainties in the least significant figures hereafter). Table 1 presents the timing solution of SMC X-1. Fig. 1 presents the pulse arrival times after the removal of the quadratic trend (or intrinsic $-\dot{P}$) together with the residuals of circular ($e = 0$) and eccentric orbit models, respectively.

In Table 2, we present the orbital epoch ($T_{\pi/2}$) measurements from different observatories and orbital cycle number (N). In Fig. 2, we present observed minus calculated values of orbital epochs ($T_{\pi/2} - n\langle P_{\rm orbit}\rangle - \langle T_{\pi/2} - n\langle P_{\rm orbit}\rangle\rangle$) relative to the constant orbital period ($\langle P_{\rm orbit}\rangle = 3.892188$ d). It should be noted that the rightmost point indicated as '*RXTE* Point' is our result and other points were already published before (see fig. 7 in Wojdowski et al. 1998). A quadratic fit to the epochs from all experiments yielded an estimate of the rate of period change $\dot{P}_{\rm orb}/P_{\rm orb} = -3.402(7) \times 10^{-6}\,{\rm yr}^{-1}$.

3.2 Pulse period history

For the other observations between MJD 500 93 and MJD 529 88 (each having ∼1–2 ks exposure), we roughly obtained pulse periods using the periodogram and then refined these periods by the use of a linear fit to the arrival times. Errors were estimated using the scattering of arrival time values (i.e. errors were related to the errors of the linear coefficient of the fit). These periods were corrected for the binary motion of the pulsar using the orbital parameters listed

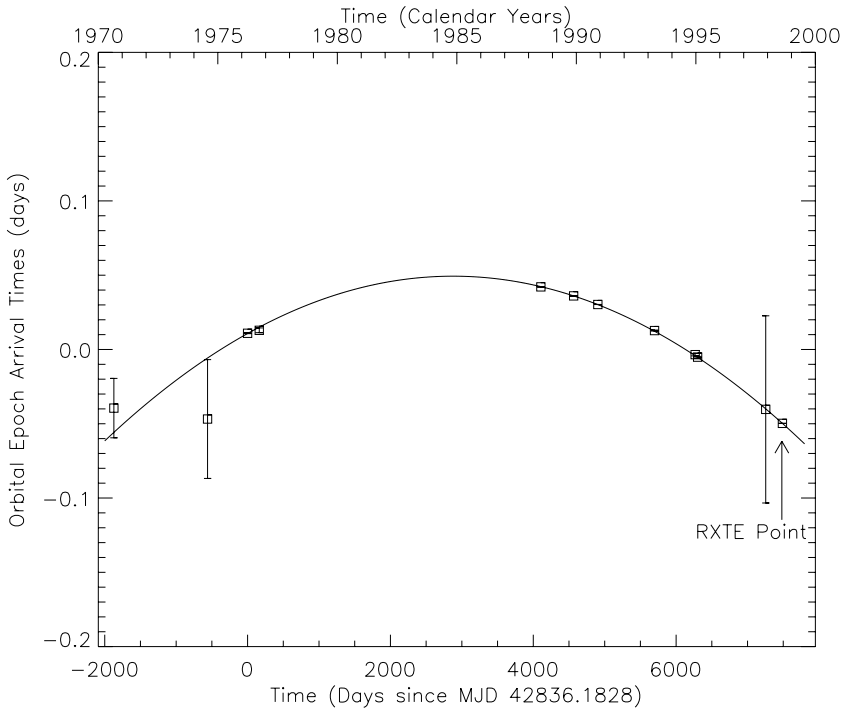


Figure 2. Orbital epoch arrival times of SMC X-1 with a time-span of about 30 yr. From the quadratic fit to the data, an orbital period decay with $\dot{P}_{\rm orbit}/P_{\rm orbit} = -3.402(7) \times 10^{-6}\,{\rm yr}^{-1}$ is found.

Downloaded from https://academic.oup.com/mnras/article-abstract/403/1/378/1018921 by Middle East Technical University Library user on 24 July 2020

Table 3. Pulse frequency history of SMC X-1.

Proposal ID or observatory	MJD (d)	Pulse period[1]	References
Uhuru	411 14.200	1.39377(51)	Henry & Schrier (1977)
Aerobee	419 99.600	1.3959(4)	Yentis et al. (1977)
Apollo-Soyuz	426 13.799	1.3982(8)	Henry & Schrier (1977)
SAS-3	428 36.183	1.3988247(1)	Wojdowski et al. (1998)
Ariel V	429 99.6567	1.3991225(23)	Wojdowski et al. (1998)
Einstein	439 85.907	1.401180(63)	Wojdowski et al. (1998)
EXOSAT	459 98.500	1.4052680772(8)	Kunz et al. (1993)
Ginga	469 42.4724	1.407277083(71)	Levine et al. (1993)
HEXE	473 99.500	1.4081806(29)	Kunz et al. (1993)
Ginga	474 01.744	1.408171707(30)	Levine et al. (1993)
HEXE	474 51.500	1.4082567(30)	Kunz et al. (1993)
HEXE	475 91.000	1.4085229(30)	Kunz et al. (1993)
Ginga	4774.3591	1.408827913(64)	Levine et al. (1993)
ROSAT 1	485 34.3479	1.41021063(68)	Wojdowski et al. (1998)
ROSAT 2	488 92.4191	1.4108022(12)	Wojdowski et al. (1998)
ASCA	491 02.5911	1.4111556(18)	Wojdowski et al. (1998)
ROSAT 3	491 37.6191	1.4112350(10)	Wojdowski et al. (1998)
ROSAT	500 54.000	1.41305(12)	Kahabka & Li (1999)
RXTE	500 91.170	1.41308143(16)	Wojdowski et al. (1998)
00011	500 93.048	1.4130802(13)	This paper
00011	500 93.115	1.4130802(39)	This paper
00011	500 93.181	1.4130786(14)	This paper
10139	503 23.016	1.41361728(15)	This paper
10139	503 23.349	1.4136112(52)	This paper
10139	503 24.010	1.413626129(76)	This paper
10139	503 25.069	1.41362903(34)	This paper
10139	503 26.009	1.413627028(64)	This paper
10139	503 27.268	1.4136316(18)	This paper
10139	503 27.941	1.413637100(64)	This paper
10139	503 28.993	1.413640077(64)	This paper
10139	503 29.940	1.413637060(64)	This paper
20146-20109-20417	504 11.87	1.413823(17)	This paper
20146-20109-20417	504 42.90	1.413918(16)	This paper
BeppoSAX-1	504 60.900	1.413971(16)	Naik & Paul (2004)
20146-20109-20417	504 89.366	1.4140261(14)	This paper
20146-20109-20417	505 04.524	1.4140567(16)	This paper
20146-20109-20417	505 05.169	1.4140587(18)	This paper
BeppoSAX-2	505 07.600	1.414067(8)	Naik & Paul (2004)
20146-20109-20417	505 31.806	1.4141297(10)	This paper
20146-20109-20417	505 35.679	1.4141399(14)	This paper
20146-20109-20417	505 51.398	1.4141789(10)	This paper
20146-20109-20417	505 56.346	1.414180(15)	This paper
BeppoSAX-3	505 62.100	1.414199(14)	Naik & Paul (2004)
20146-20109-20417	505 66.861	1.4142307(9)	This paper
20146-20109-20417	505 79.511	1.414251(16)	This paper
20146-20109-20417	505 83.009	1.4142586(5)	This paper
20146-20109-20417	505 83.030	1.4142597(14)	This paper
ROSAT	505 93.799	1.41430(2)	Kahabka & Li (1999)
20146-20109-20417	505 97.960	1.414306(2)	This paper
20146-20109-20417	505 98.980	1.4143059(14)	This paper
20146-20109-20417	506 09.319	1.414340(5)	This paper
20146-20109-20417	506 17.757	1.4143399(96)	This paper
20146-20109-20417	506 17.898	1.41433(5)	This paper
20146-20109-20417	506 46.787	1.414420(7)	This paper
20146-20109-20417	506 75.866	1.414488(13)	This paper
20146-20109-20417	507 11.833	1.41457(2)	This paper
20146-20109-20417	507 38.053	1.414631(10)	This paper
20146-20109-20417	507 67.442	1.414706(10)	This paper
20146-20109-20417	507 95.116	1.41477(7)	This paper
30125	508 50.541	1.414891(5)	This paper
30125	508 83.272	1.41497(2)	This paper
ROSAT	508 98.200	1.41501(2)	Kahabka & Li (1999)
30125	509 10.965	1.4150(2)	This paper
30125	509 49.407	1.415116(5)	This paper

Downloaded from https://academic.oup.com/mnras/article-abstract/403/1/378/1018921 by Middle East Technical University Library user on 24 July 2020

Table 3 – *continued*

Proposal ID or observatory	MJD (d)	Pulse period[1]	References
30125	509 49.751	1.41512(6)	This paper
30125	509 50.048	1.415128(11)	This paper
30125	510 07.374	1.41524(6)	This paper
30125	510 07.975	1.415242(7)	This paper
30125	510 60.725	1.41538(5)	This paper
30125	510 60.791	1.41538(4)	This paper
30125	510 61.265	1.415376(18)	This paper
30090-30125	511 02.221	1.41548(9)	This paper
30090-30125	511 06.083	1.41548(2)	This paper
30090-30125	511 08.060	1.415432(18)	This paper
30090-30125	511 09.781	1.41543(3)	This paper
30090-30125	511 11.866	1.41544(2)	This paper
30090-30125	511 13.711	1.415443(4)	This paper
30090-30125	511 15.709	1.415446(6)	This paper
30090-30125	511 17.607	1.415451(20)	This paper
30090-30125	511 19.586	1.415455(4)	This paper
30090-30125	511 21.160	1.415509(2)	This paper
30090-30125	511 21.515	1.4155127(14)	This paper
30090-30125	511 21.637	1.41552(11)	This paper
30090-30125	511 21.724	1.41551(4)	This paper
30090-30125	511 25.443	1.41552(7)	This paper
30090-30125	511 27.234	1.415528(17)	This paper
30090-30125	511 29.376	1.41553(10)	This paper
30090-30125	511 31.300	1.41553(5)	This paper
30090-30125	511 33.301	1.41555(6)	This paper
30090-30125	511 51.014	1.41559(3)	This paper
30090-30125	511 51.416	1.41558(3)	This paper
40064	516 99.405	1.416816(9)	This paper
40064	516 99.666	1.416824(9)	This paper
40064	516 99.736	1.41681(3)	This paper
40064	516 99.876	1.416812(16)	This paper
40064	517 00.172	1.41681(6)	This paper
40064	517 00.233	1.416809(22)	This paper
40064	517 00.383	1.416809(20)	This paper
40064	517 00.593	1.41681(9)	This paper
40064	517 00.663	1.416808(47)	This paper
40064	517 00.803	1.416810(14)	This paper
40064	517 00.896	1.416807(57)	This paper
40064	517 01.152	1.416814(45)	This paper
40064	517 01.315	1.416817(3)	This paper
40064	517 01.590	1.41682(13)	This paper
40064	517 01.660	1.416819(43)	This paper
40064	517 01.869	1.416822(33)	This paper
40064	517 01.957	1.4168218(3)	This paper
Chandra	518 33.808	1.4170032(6)	Vrtilek et al. (2005)
INTEGRAL	528 43	1.419253(16)	McBridge et al. (2007)
80078	529 39.611	1.419470(5)	This paper
80078	529 39.680	1.419472(6)	This paper
80078	529 39.749	1.4194708(19)	This paper
80078	529 40.527	1.4194728(50)	This paper
80078	529 40.596	1.419473(34)	This paper
80078	529 40.665	1.41947(3)	This paper
80078	529 40.734	1.4194722(15)	This paper
80078	529 40.805	1.419471(3)	This paper
80078	529 40.958	1.419470(13)	This paper
80078	529 41.304	1.419468(50)	This paper
80078	529 41.373	1.419465(38)	This paper
80078	529 41.442	1.419464(36)	This paper
80078	529 41.511	1.419464(11)	This paper
80078	529 41.813	1.419460(4)	This paper
80078	529 42.289	1.419462(2)	This paper
80078	529 42.565	1.419466(33)	This paper
80078	529 42.652	1.419469(76)	This paper
80078	529 42.825	1.41947(28)	This paper

Downloaded from https://academic.oup.com/mnras/article-abstract/403/1/378/1018921 by Middle East Technical University Library user on 24 July 2020

Table 3 – *continued*

Proposal ID or observatory	MJD (d)	Pulse period[1]	References
80078	529 42.891	1.41947(35)	This paper
80078	529 43.688	1.419481(6)	This paper
80078	529 81.226	1.4195(4)	This paper
80078	529 81.527	1.41955(13)	This paper
80078	529 82.064	1.419578(10)	This paper
80078	529 83.496	1.41958(3)	This paper
80078	529 84.033	1.419572(6)	This paper
80078	529 84.360	1.419570(45)	This paper
80078	529 84.480	1.419567(36)	This paper
80078	529 84.687	1.419566(12)	This paper
80078	529 84.890	1.419566(16)	This paper
80078	529 85.326	1.419571(7)	This paper
80078	529 86.311	1.419586(25)	This paper
80078	529 87.433	1.419587(39)	This paper
80078	529 87.640	1.419585(43)	This paper

[1]errors indicated in the parenthesis give the value for each pulse period in 1σ.

in Table 1. We present the whole pulse period history of the source in Table 3 and Fig. 3 including our results. From Fig. 3, it is evident that the source spins up continuously between MJD ∼400 00 and ∼530 00 with a varying spin-up rate. In Table 4, average spin-up rate values of the source are listed.

4 SPECTRAL ANALYSIS

The same 130 *RXTE*-PCA observations used for the timing study were also used for the spectral analysis except those between 1998 October 16 and November 24 which were contaminated due to the outburst of the nearby transient X-ray pulsar XTEJ0111.2-7317 (Chakrabarty et al. 1998). We used the Standard-2 mode data, which provide 128 channel spectra at 16 s time resolution. Spectrum, background and response matrix files were created using FTOOLS 6.3 data analysis software. We used background-subtracted spectra in our analysis. Energy channels corresponding to the 3–25 keV energy range were used to fit the spectra. We ignored photon energies lower than 3 keV and higher than 25 keV and 1 per cent systematic error was added to the errors (see Wilms et al. 1999; Coburn et al. 2000).

To fit the spectra, we used a power-law model with a high-energy cut-off and a Gaussian component peaking at 6.7 keV (Angelini, Stella & White 1991). We also tried to add a partial covering absorption component (Neilsen, Hickox & Vrtilek 2004), but adding this model component did not improve the fit.

Table 5 shows best-fitting parameters of the spectral model for two sample observations. In general, we found that power-law index, high-energy cut-off and e-fold energy does not show variations with time, orbital phase and X-ray flux within the errors. We found that Hydrogen column density gets higher when X-ray flux is lower (see Fig. 4).

5 DISCUSSION

In this paper, we presented timing and spectral analysis of *RXTE*-PCA observations of SMC X-1 with a time-span of about 8 yr. From timing analysis, we revised timing solution of the source and resolved an eccentricity value. We also confirmed the orbital decay reported before. Our timing analysis helped us to construct a ∼30 yr long pulse period history of the source (see Fig. 3). From the spectral analysis, we found that all spectral parameters except Hydrogen column density showed no significant variation with time and X-ray flux.

Fig. 1 demonstrates that the eccentric orbit model is a better fit compared to the circular orbital model. The timing solution of the source revealed that the binary orbit has an eccentricity of 0.00089(6). Wojdowski et al. (1998) had found a circular orbit solution and Levine et al. (1993) had only found an upper limit of 0.00004 for eccentricity. Our present value is more than 20 times greater than the upper limit found by Levine et al. (1993). This significant eccentricity value should be verified using future monitoring observations.

From timing analysis, we obtained a new orbital epoch of SMC X-1 from *RXTE* observations. Using this new epoch and previous results (Wojdowski et al. 1998), we found that there is an orbital decay with $\dot{P}_{\rm orbit}/P_{\rm orbit}$ of $-3.402(7) \times 10^{-6}\,{\rm yr}^{-1}$. This value is similar to the values found by Wojdowski et al. (1998) and Levine et al. (1993). Levine et al. (1993) proposed that the major cause of change in the orbital period is tidal interactions as for the case in Cen X-3 (Kelley et al. 1983) and LMC X-4 (Levine, Rappaport & Zojcheski 2000). SMC X-1 is unlike Her X-1 for which the mass accretion was thought to be primarily related to the orbital period decay (Deeter et al. 1991).

From Fig. 3, it is seen that SMC X-1 spins up continuously for ∼30 yr. We found that average long-term spin-up rate of the source between MJD 500 93.048 and 529 87.640 (whole time-span of our analysis) is $2.65343816(7) \times 10^{-11}\,{\rm Hz\,s^{-1}}$.

Spin-up rate of a source with a persistent accretion disc can be expressed as

$$\dot{\nu} \simeq 2.2 \times 10^{-12} \mu_{30}^{2/7} m_x^{-3/7} R_6^{6/7} I_{45}^{-1} L_{37}^{6/7}\,{\rm Hz\,s^{-1}}, \quad (3)$$

where $\dot{\nu}$ is first time derivative of the spin frequency, μ_{30} is the magnetic moment of the neutron star in units of $10^{30}\,{\rm G\,cm^3}$, m_x is the mass of the neutron star in units of solar mass, R_6 is the radius of the neutron star in units of cm, I_{45} is the moment of inertia of the neutron star in terms of $10^{45}\,{\rm g\,cm^2}$ and L_{37} is the luminosity of the neutron star in units of $10^{37}\,{\rm erg\,s^{-1}}$ (Ghosh & Lamb 1979). Using a distance value of 61 kpc (Keller & Wood 2006) and a flux of $1.2 \times 10^{-9}\,{\rm erg\,cm^{-2}\,s^{-1}}$ (see Fig. 4), luminosity of SMC X-1 is $\sim 5.5 \times 10^{38}\,{\rm erg\,s^{-1}}$. Assuming magnetic moment of $10^{30}\,{\rm G\,cm^3}$, mass of $1.4\,{\rm M_\odot}$, radius of 10^6 cm, moment of inertia of $10^{45}\,{\rm g\,cm^2}$, we find $\dot{\nu}$ to be $\sim 5.9 \times 10^{-11}\,{\rm Hz\,s^{-1}}$. This value is of the order of the observed spin-up rate value of the source.

© 2010 The Authors. Journal compilation © 2010 RAS, MNRAS **403,** 378–386

Downloaded from https://academic.oup.com/mnras/article-abstract/403/1/378/1018921 by Middle East Technical University Library user on 24 July 2020

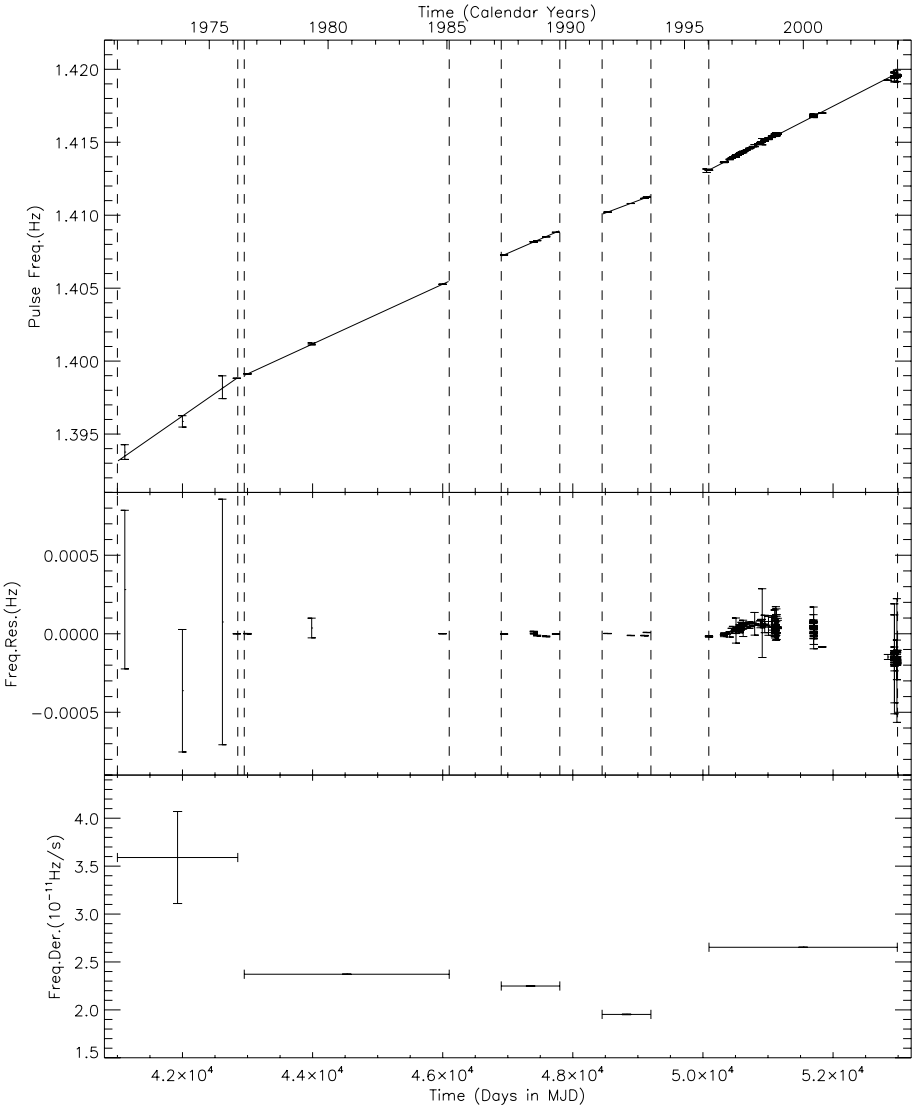


Figure 3. (top) and (middle) Pulse frequency history and residuals of SMC X-1 after a linear fit obtained from five different intervals listed in Table 4. (bottom) Frequency derivative history. Dashed lines in top and middle panels and horizontal error bars in the bottom panel indicate time intervals in which linear fits were performed. The last (rightmost) interval almost consists of pulse frequency values obtained from our analysis.

Table 4. Long-term spin-up rate values of SMC X-1.

Interval (MJD–MJD)	Spin-up rate (10^{-11} Hz s^{-1})
410 00–428 50	3.59(48)
429 50–461 00	2.3718(15)
469 00–478 00	2.2491438(1)
484 50–492 00	1.9528(38)
500 93–529 88	2.65343816(7)

From Fig. 3 and Table 4, it is evident that the long-term spin-up rate of SMC X-1 varies within a factor of 2. From equation (3), this variation may – in principle – be related to a change in X-ray luminosity of the source. However, previous X-ray observations of the source were performed by different X-ray observatories and/or in different energy bands. These observations are sparsely distributed and average X-ray flux of these observations are not likely to represent an average X-ray flux for the intervals for which the pulse frequency derivatives were found. Moreover, X-ray flux variations are also affected by the super-orbital cycle, period of which is not as stable as that of Her X-1 (Clarkson et al. 2003). Therefore, it is not possible to test whether variation in long-term spin-up rate is related to a change in X-ray luminosity or not.

From Table 1, spin-up rate obtained from ∼6 d long observation around MJD 503 24.7 is 3.279(5) × 10^{-11} Hz s^{-1}. This is about 20 per cent greater than the long-term spin-up rate between MJD 500 93 and 529 88. Assuming that the pulse frequency variations can be explained in terms of random walk model in pulse frequency (Baykal & Ogelman 1993), one can express the pulse frequency derivative variations as $\langle \Delta\dot{\Omega}^{1/2} \rangle = \sqrt{\frac{S}{t}}$, where S is the noise strength and t is the time interval at which the pulse frequency derivatives are observed. Therefore, it is natural to observe high pulse frequency derivative fluctuations at shorter time-scales. It is important to note that we refined pulse period values fitting arrival times each obtained from ∼200 s long intervals; therefore, we had to have at least a few arrival times to obtain spin period accurately. So, our shortest time-scale to obtain pulse periods is of the order of a single *RXTE* observation which is ∼1–2 ks long.

Downloaded from https://academic.oup.com/mnras/article-abstract/403/1/378/1018921 by Middle East Technical University Library user on 24 July 2020

Table 5. Sample spectral parameters from two different observations.

Obs ID	10139-01-01-00	20146-06-02-00
MJD	503 23.349	504 42.905
nH (10^{22} cm^{-2})	12.039 ± 0.748	2.214 ± 0.290
Power-law Index	1.184 ± 0.043	1.176 ± 0.074
$E_{\rm cut-off}$(keV)	13.697 ± 3.424	6.595 ± 1.649
$E_{\rm fold}$ (keV)	11.765 ± 4.118	10.020 ± 3.507
(χ^2_ν) (degrees of freedom)	0.868(47)	1.055(47)
Observed flux (10^{-10} erg cm^{-2} s^{-1})(3–25 keV)	$2.3866^{+0.0282}_{-0.102}$	$20.673^{+0.043}_{-0.157}$
Unabsorbed flux (10^{-10} erg cm^{-2} s^{-1})(3–25 keV)	$2.8281^{+0.002}_{-0.012}$	$21.553^{+0.039}_{-0.078}$

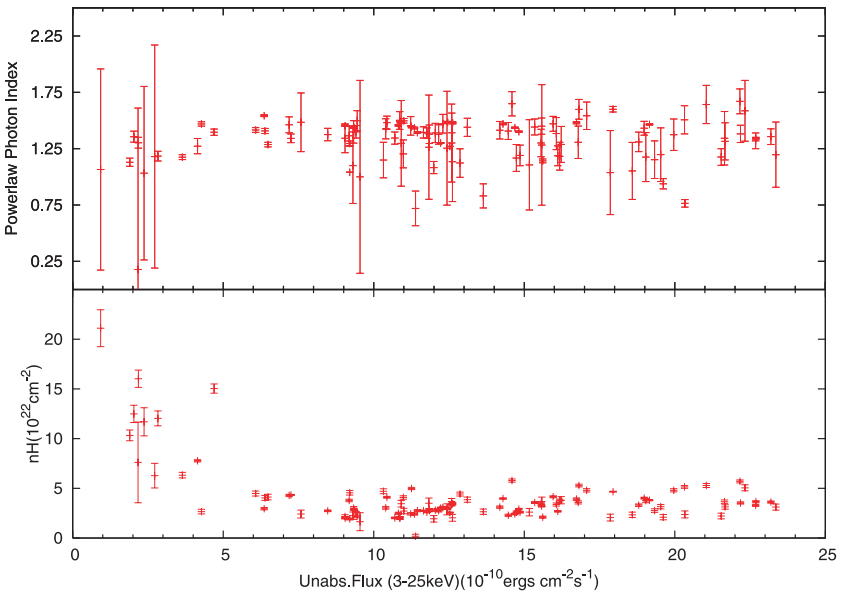


Figure 4. Dependence of photon index and n_H on 3–25 keV unabsorbed X-ray flux.

From the spectral analysis, we found that all of the spectral parameters except Hydrogen column density did not vary significantly. Hydrogen column density was found to be higher as X-ray flux gets lower. Increase in Hydrogen column density with a decrease in X-ray flux is also observed in Her X-1 (Inam & Baykal 2005) and may be due to the fact that soft absorption becomes stronger whenever there is a partial obscuration of the neutron star due to the X-ray eclipses and warping of the accretion disc. The increase in Hydrogen column density may also be an artefact of the simple absorbed power-law model. Paul et al. (2002) showed that SMC X-1 has soft excess especially for energies $\lesssim$3 keV. Although we used photon energies greater than 3 keV in our analysis, tail of a soft spectral component may affect low energies in our analysis and as a result we might have misidentified corresponding changes in energy spectrum as variations in Hydrogen column density parameter.

ACKNOWLEDGMENTS

We acknowledge support from EU FP6 Transfer of Knowledge Project 'Astrophysics of Neutron Stars' (MTKD-CT-2006-042722).

REFERENCES

Angelini L., Stella L., White N. E., 1991, ApJ, 371, 332
Baykal A., Ogelman H., 1993, A&A, 267, 119
Bonnet-Bidaud J. M., van der Klis M., 1981, A&A, 97, 134
Chakrabarty D., Levine A. M., Clark G. W., Takeshima T., 1998, Int. Astron. Union Circular, 7048, 1
Clarkson W. I., Charles P. A., Coe M. J., Laycock S., Tout M. D., Wilson C. A., 2003, MNRAS, 339, 447
Coburn W. et al., 2000, ApJ, 543, 351
Davison P. J. N., 1977, MNRAS, 179, 15
Deeter J. E., Boynton P. E., 1985, in Hayakawa S., Nagase F., eds, Proc. Inuyama Workshop on Timing Studies of X-Ray Sources. Nagoya Univ., Nagoya, p. 29
Deeter J. E., Boynton P. E., Pravdo S. H., 1981, ApJ, 247, 1003
Deeter J. E., Boynton P. E., Miyamoto S., Kitamoto S., Nagose R., Kawar N., 1991, ApJ, 383, 324
Galache J. L., Corbet R. H. D., Coe M. J., Laycock S., Schurch M. P. E., Markwardt C., Marshall F. E., Lochner J., 2008, ApJS, 177, 189
Ghosh P., Lamb F. K., 1979, ApJ, 234, 296
Gruber D. E., Rothschild R. E., 1984, ApJ, 283, 546
Henry P., Schrier E., 1977, ApJ, 212, L13
Inam S. C., Baykal A., 2005, MNRAS, 361, 1393
Jahoda K., Swank J. H., Giles A. B., Stark M. J., Strohmayer T., Zhang W., Morgan E. H., 1996, Proc. SPIE, 2808, 59
Kahabka P., Li X. D., 1999, A&A, 345, 117
Keller S. C., Wood P. R., 2006, ApJ, 642, 834
Kelley R. L., Rappaport G., Clark G. W., Petro L. D., 1983, ApJ, 268, 790
Kunz M. et al., 1993, A&A, 268, 116
Levine A., Rappaport S., Deeter J. E., Boynton P. E., Nagase F., 1993, ApJ, 410, 328
Levine A. M., Rappaport S. A., Zojcheski G., 2000, ApJ, 541, 194

Downloaded from https://academic.oup.com/mnras/article-abstract/403/1/378/1018921 by Middle East Technical University Library user on 24 July 2020

Lucke R., Yentis D., Friedman H., Fritz G., Shulman S., 1976, ApJ, 206, L25
McBridge V. A. et al., 2007, MNRAS, 382, 743
Naik S., Paul B., 2004, A&A, 418, 655
Neilsen J., Hickox R. C., Vrtilek S. D., 2004, ApJ, 616, L135
Paul B., Nagase F., Endo T., Dotani T., Yokogawa J., Nishiuchi M., 2002, ApJ, 579, 411
Price R. E., Groves D. J., Rodrigues R. M., Seward F. D., Swift C. D., Toor A., 1971, ApJ, 168, L7
Primini F. A. 1977, PhD thesis, submitted to Massachusetts Institute of Technology
Reynolds A. P., Hilditch R. W., Bell S. A., Hill G., 1993, MNRAS, 261, 337
Schreier E., Giacconi R., Gursky H., Kellogg E., Tananbaum H., 1972, ApJ, 178, L71
Trowbridge S., Nowak M. A., Wilms J., 2007, ApJ, 670, 624
Tuohy I. R., Rapley C. G., 1975, ApJ, 198, L69
van der Meer A., Kaper L., van Kerkwijk M. H., Heemskerk M. H. M., van den Heuvel E. P. J., 2007, A&A, 473, 523
Vrtilek S. D., Raymond J. C., Boroson B., McCray R., 2005, ApJ, 626, 307
Wilms J., Nowak M. A., Dove J. B., Fender R. P., di Matteo T., 1999, ApJ, 522, 460
Wojdowski P., Clark George W., Levine Alan M., 1998, ApJ, 502, 253
Yentis D., Shulman S., Mckee J. D., Rose W. K., 1977, Astrophys. Lett., 19, 53

This paper has been typeset from a TEX/LATEX file prepared by the author.

Downloaded from https://academic.oup.com/mnras/article-abstract/403/1/378/1018921 by Middle East Technical University Library user on 24 July 2020